2010 21st International Lightning Detection Conference
19 – 20 April • Orlando, Florida, USA
3rd International Lightning Meteorology Conference
21 – 22 April • Orlando, Florida, USA

DETECTION EFFICIENCY OF THE TOHOKU IMPACT SENSOR NETWORK IN WINTER

Noriyasu Honma
Tohoku Electric Power Company
Sendai, Japan

1. INTRODUCTION

In the Tohoku region of Japan, a lightning location system (LLS) has been operated by the Tohoku Electric Power Company since 1994. This system consists of nine IMPACT sensors set at medium gain with the threshold cut down to half of the standard level. This expands the detection range to a distance comparable to a high-gain sensor. The configuration enables the LLS to detect lightning electromagnetic pulses (LEMP's) of magnitudes corresponding to peak currents from 10 to 300 kA within the observation area.

This system has been providing valuable information to the company to help it quickly identify transmission line (TL) faults caused by lightning. Lightning frequency statistics based on accumulated location data have been used to guide rational investment in electrical facility design for lightning tolerance. For lightning flashes causing TL fault in winter, however, the detection efficiency (DE) has been lower than that in summer. Solving this problem has been a high priority, not only because of the expense required to investigate and confirm lightning caused faults, but also for public safety.

To investigate the cause of the lower DE of the Tohoku LLS in winter, observations of LEMP's in the region were conducted using a fast antenna (FA) network. Some characteristic waveforms were found by analyzing the observed LEMP waveforms associated with lightning events that caused TL faults. Their characteristics were different from those commonly observed in summer lightning. Similar lower DE for the LLS networks in other coastal areas of the Sea of Japan has also been reported.

This paper presents the DE of the Tohoku LLS in winter, the characteristics of the LEMP waveforms associated with the lower DE, and some observations regarding the features of winter lightning.

2. OBSERVATION AND DATA

2.1 LEMP Observations

LEMP waveforms were recorded with two types of FA having time precision of 200 ns using a GPS clock. The observation frequency of both types ranged from about 700 Hz to 1 MHz. The electric field was digitized at a rate of 12 bits for every 200 ns and recorded for 1.6 ms in each frame. This type of recording system can be triggered successively up to 15 times without substantial dead time. The network of five lower gain FA's (FA-N1 to FA-N5) surrounds an area also observed by still cameras near the coast of the Sea of Japan as shown in Figure 1. The FA-N network is effective not only in investigating the fine structure of the LEMP waveforms associated with the lightning discharges in this area, but also in detecting LEMP's of large amplitude.

The FA-D network (FA-D1 to FA-D4) has two channels. LEMP waveforms are digitized at a rate of 12 bits every 1 μs and recorded for 8 ms in each frame without dead time for up to two sets of 15 frames in the master channel. They are then digitized at 12 bits every 100 ns and recorded for 0.8 ms in the slave channel at the same trigger time. The master channel has the role to record the most

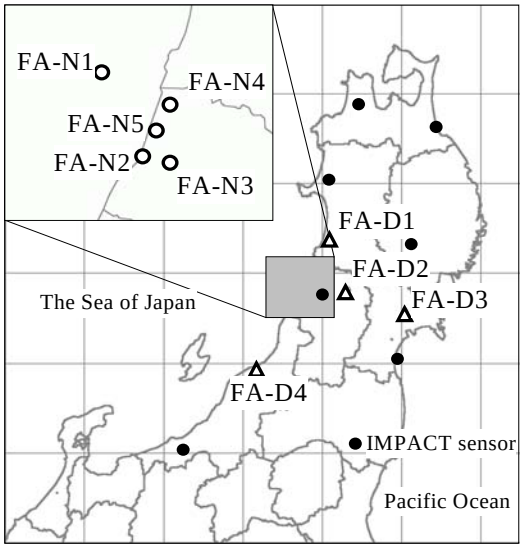

Figure 1. Configuration of the IMPACT sensor network and the FA networks in the Tohoku region of Japan.

significant LEMP waveforms to investigate the overall features of lightning discharges. The slave channel records the main LEMP waveform with a higher time resolution. The FA-D network enables it to record radiation fields associated with lightning causing TL faults and estimates their locations in the entire Tohoku region efficiently.

2.2 Calibration of the FA

The FAs are calibrated to the same gain in each type of FA-N and FA-D. The upper observation frequency of 1 MHz, however, is higher than the 350 kHz frequency of an IMPACT sensor. This difference enhances the peak current estimated from the peak field having the higher frequency components recorded by the FA. It also introduces variations in the peak current estimate caused by propagation effects related to the distance from the lightning to the FA. The final peak current for this analysis is the average of the estimated value after truncation by discarding values that deviate from the mean by more than 20%.

The method used for peak current estimates in the LLS is based on the TL model. However, the LEMP radiation mechanism characteristic in winter lightning has not been clarified yet. For that reason, the calibration method described in the paragraph above is used to estimate an index of the peak current amplitude from the peak field measurements in this paper.

2.3 Correlation of LEMP data with TL faults

Most of the TL fault data has been recorded with an accuracy of about 1 minute. Most of the field waveforms associated with the lightning that occurred in the investigated region have been observed. Therefore, the LEMP waveform related to the fault can be identified by confirming the coincidence of the location, the features of the waveform and the peak current.

For more than half of the TL faults, the locations have been confirmed by traces on the arcing horns or by a fault location system. Those locations have been compared with the radiation source of the LEMP located by the time-of-arrival (TOA) method. The allowed timing error was about 3 μs considering the effect on the LEMP waveform of propagation over land. The selected LEMP waveforms had peak amplitudes corresponding to the peak currents that were large enough to cause TL faults.

In the same manner, the location data of the LLS was correlated with the TL faults.

3. ANALYSIS

3.1 Classification of LEMP waveforms

Characteristic LEMP waveforms observed in the Hokuriku region in winter were investigated and classified by Ishii as follows. These waveforms are thought to be associated with lightning discharges in which a charge in the cloud descends to the ground through a leader channel that has progressed upward from a ground-based object.

In case of negative charge in the cloud, a positive leader progresses upward into the negatively charged region and connects to the other discharge channel, according to the model proposed by Miyazaki and Ishii. This type of discharge is classified as a negative ground-to-cloud (-GC) stroke and radiates a LEMP characterized by a bipolar pulse series whose first half cycle is of positive polarity. The main bipolar pulse around the end of the pulse series has the largest amplitude, longer rise time, shorter zero-crossing time, and larger bipolarity without fast transition on the rising portion.

Positive ground-to-cloud (+GC) strokes, guided by the negative leader progressing from the ground in a manner similar to the –GC stroke, are classified as +GC stroke of Types I or II (+GC I or +GC II). There is not much difference between the LEMP waveforms for +GC Type II strokes and normal cloud-to-ground (CG) strokes that carry in-cloud positive charge to the ground without pulses around the main pulse. For +GC Type I, the main pulse is relatively calm and has a longer rise time than that of a +GC II stroke.

LEMP waveforms observed in the Tohoku region have been sorted using these classifications. Based on the analysis of observed waveforms, the LEMP waveform for a typical +CG stroke is presumed to have the following characteristics. The main pulse has a smooth concave front. In addition, continuous noisy field changes prior to the main pulse are less than 3% of the main peak in amplitude. This discrimination concept has, however, an ambiguity because the investigation of noise depends on the background noise conditions, and fine field changes in higher frequency are hard to observe from distant sites due to the propagation effect.

3.2 DE of LLS in winter

During three consecutive winter seasons beginning in October 2002, 2003 and 2004, LEMP waveforms associated with flashes were correlated with 95 out of 124 TL faults having confirmed locations. Among these samples representing half of the 189 total faults, 59 lightning flashes were detected by the Tohoku LLS, which corresponds to 62% DE in the three winter seasons. The evaluation of DE is summarized in Table 1.

Table 1 Detection efficiency of theTohoku LLS for lightning flashes causing TL faults in winter.

Year	2002	2003	2004	Total
Total number	29	38	28	95
Detected number	20	23	16	59
Rejected number	9	15	12	36
DE [%]	69	61	57	62

These statistics are contaminated, however, by the kind of erroneous outputs summarized in Table 2. For three negative flashes, the first strokes are rejected and the second strokes are misinterpreted as first strokes. For two other negative flashes, the polarities of the main pulses for the first stroke disagree with those observed by the LLS, but the causes cannot be determined from the field waveforms. For one positive flash, the peak current estimated by the LLS is much smaller than the estimate from the corresponding peak field.

Table 2 Erroneous outputs of the Tohoku LLS for lightning flashes and their discharge types in the same winter season as Table 1.

Erroneous outputs of LLS	Discharge type	Number
Rejection of 1st stroke	-GC	3
Disagreement of polarity	-GC	2
Disagreement of peak current	+GC II	1
Total number		6

Fig. 2 (a) shows a sample electric field change recorded at a distance of about 100 km from a fault on a 66 kV TL. The electric field change begins with a pulse series followed by a bipolar pulse with occurring in a time period of about 1 ms. From the characteristics of the waveforms and their polarity, the initial pulses are believed to be associated with the preliminary breakdown (PB) and the following bipolar pulse is thought to be the return stroke (RS) of a negative cloud-to-ground (–CG) stroke. About 300 ms after the first stroke, an asymmetric pulse of the same polarity as the first one was observed. This pulse is thought to be associated with a –CG stroke from the characteristics of the waveform such as the steep rate of rise and the small bipolarity.

Based on the arrival time of the LEMP's, the first –CG stroke is located where the TL fault occurred and the corresponding peak current is estimated at –63 kA, enough to cause the TL fault. However, it was not located by the LLS. On the other hand, the following –CG stroke is about 4 km away from the TL fault and the corresponding peak current is about –27 kA, which coincides with the location data from the LLS. This situation might lead the LLS user to misunderstand the cause of the fault. He might think the second –CG stroke struck the conductor of the TL, but was located by the LLS with large error because, for example, the lightning stroke was outside the sensor network where location accuracy is lower.

The rejection of the first stroke pulse may be because the bipolarity was larger than the 1.0 value set in the first version of the IMPACT sensor. Another possible reason is the short time interval between the large preceding pulses in comparison to the 4 ms dead time during waveform processing in the sensor.

The sample waveform shown in Figure 2 (b) consists of a bipolar pulse series, a large bipolar pulse and two isolated asymmetric pulses sequentially. The first pulse of the bipolar pulse series is asymmetric, before which no field change is observed. The subsequent pulses are bipolar with larger amplitudes than the first one. The peak amplitudes of the subsequent pulses increase and then decrease. Those polarities are the same at least in the beginning of the initial pulse series as the polarities of the large pulse that follows. The characteristics of those pulse series coincide well with that for a PB, which implies that this kind of discharge should be classified as a –GC stroke.

The largest bipolar pulse has a peak amplitude corresponding to a peak current of -142 kA and is located near the TL fault. The subsequent pulses have features that are similar to subsequent pulses of a normal –CG stroke. Therefore, those strokes are presumed to be a multiple stroke flash triggered by an upward leader. The first stroke, however, was not located, and the first subsequent stroke was misinterpreted by the LLS as the first stroke causing TL fault.

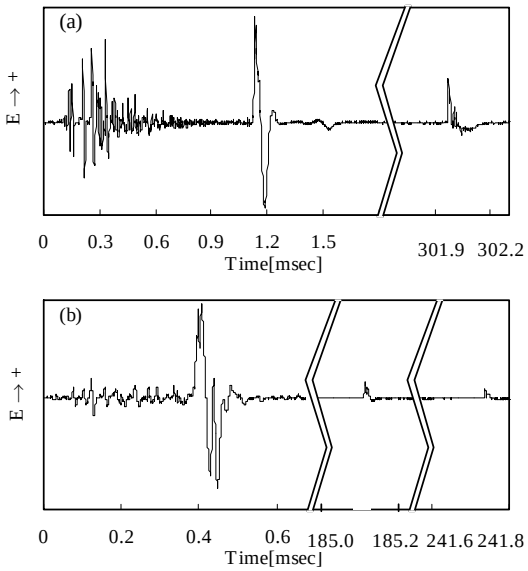

Fig. 2 Sample field waveforms associated with negative flashes. (a) IMPACT sensors rejected the main largest pulse whose peak current is estimated to be -63kA, but detected the other strokes about 4 km away from the rejected stroke. (b) IMPACT sensors rejected the main largest pulse whose peak current is estimated to be –142kA, but detected the subsequent strokes.

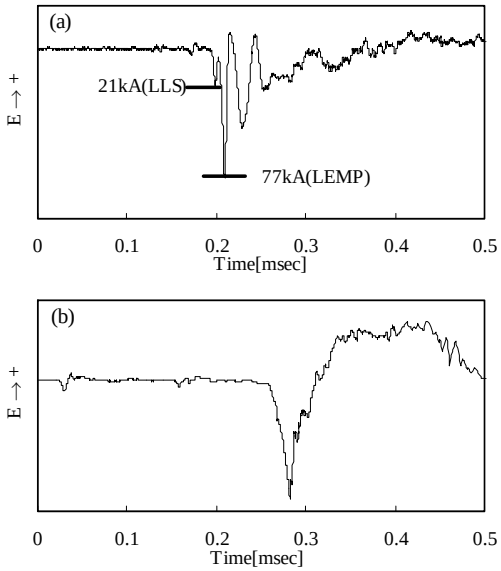

Fig. 3 Sample field waveforms associated with +GC strokes superimposed by irregular field changes. (a) A small peak on the rising portion of the main pulse is misinterpreted as the main peak by the IMPACT sensor. (b) Two sets of isolated negative pulses exist prior to the main pulse with a concave front seen for general +CG stroke.

The waveform characteristics of the large bipolar pulse related to the rejection by the sensor are the larger bipolarity, the shorter zero-crossing time and the preceding pulses just prior to the main pulse.

As mentioned above, the LLS rejected the main field pulses associated with the lightning strokes causing TL faults. These errors do not influence the location of multiple stroke flashes. Multiplicity in winter, however, is lower, and the peak current error makes LLS users misunderstand the lightning causing the TL fault.

Fig. 3 (a) shows a sample waveform associated with a lightning stroke classified as +GC II. There is an error in estimating the peak current of the first stroke; +21 kA by the LLS instead of +77 kA estimated directly from the peak field. The error is caused by misinterpreting the pulse superimposed on the rising portion of the main pulse as the real main peak. In spite of the error, the radiation source was located near the TL fault by three sensors with enough accuracy.

The other sample of the electric field waveform shown in Fig. 3 (b) is thought to be associated with a Type I +GC stroke. Comparing the LEMP waveform of that stroke with typical +CG strokes, a concave front, which is one of the important characteristics for +CG strokes, is seen, but the rise time and zero-crossing time are longer. Irregular field changes are superimposed on the main pulse. Just prior to the main pulse, a few isolated asymmetric or bipolar pulses of the same polarity as the main one often exist. Their amplitudes are within about 10% of the maximum peak for analyzed LEMP waveforms except for the case in Fig. 3 (a).

The DE's for the five discharge types are summarized in Table 3. Considering the above errors in lightning location, the total DE for the first stroke falls to 56 %. Especially for –GC stroke, the DE is significantly lower than that for –CG stroke. For +GC strokes, the DE for Type II is slightly lower than that for +CG strokes, but Type I strokes, of which samples are few, seem to be hard to detect. GC strokes accounted for 70% of the strokes that were investigated, and rejected GC strokes also accounted for 95% of the total number of rejected strokes. This indicates that the key factor of lower

LLS DE in winter is the GC stroke.

Table 3 Detection efficiencies of the Tohoku LLS for the first strokes of different types of discharges in winter.

Discharge type	-CG	-GC	+CG	+GC II	+GC I	Total
Number	22	39	4	28	2	95
Percentage [%]	23	41	4	29	2	100
Detected number	21	9	3	20	0	53
Rejected number	1	30	1	8	2	42
DE [%]	95	23	75	71	0	56

3.3 Reason for low DE in winter

To investigate the reason why the sensor rejects the first stroke in winter, the waveform parameters of the main field pulses of 95 strokes were compared with the field waveform discrimination criteria of the sensor. Fig. 4 shows the histograms of waveform parameters of the 0-100% rise time (Tr1), 10-100% rise time (Tr2), zero-crossing time (Tz), and bipolar ratio, defined as the opposite-polarity overshoot to the initial peak (Bp), for stroke types of both polarities of CG's and GC's. In this figure, the abscissa shows the upper limit of each bin. The evaluated rejection rates of each criterion are summarized in Table 4.

Table 4 Rejection rates for the field waveform discrimination criteria of the IMPACT sensor for different types of discharges in winter.

Field waveform discrimination criteria	Discharge Type					Total
	-CG	-GC	+CG	+GC II	+GC I	
Rise time >30 [μs]	0	5	0	10	2	17
Percentage [%]	0	13	0	36	100	18
Zero-crossing time < 6 μs	1	4	0	2	0	7
Percentage [%]	5	10	0	7	0	7
Bipolar ratio>1.0	0	7	0	0	0	7
Percentage [%]	0	18	0	0	0	7
Total Number	22	39	4	28	2	95

As the overall features in winter, the rise time is longer, the zero-crossing time is shorter and the bipolar ratio is larger relative to those in summer. 17 out of the 69 GC strokes in both polarities had rise times longer than the 30 μs acceptable upper limit of the sensor. That corresponds to a rejection rate of 25%. One reason for the longer rise time for the -GC and +GC Type II discharges is the existence of pulses around the onset of the main pulse. This is because the rise times of 10-100% of the peak of investigated pulses are below the limit of the sensor, except only for a case of –GC stroke as shown in Fig. 4(b). For +GC I, however, the longer rise time is due to the original characteristics of the slow rising front.

Especially for 10 cases of –GC stroke, corresponding to 30% of the total, the amplitude of the second peak is more than 115% higher than the amplitude of the first peak. In this condition, the second peak is misinterpreted as the first, which makes the rise time longer, the zero-crossing time shorter, the peak amplitude larger, and the bipolar ratio smaller than those for the true first peak. Those parameters are not available in the return stroke model.

The zero-crossing time is shorter than in summer on average for most types of strokes, and it is shorter than the acceptable lower limit of 6 μs for 10% of –GC's and 7% of +GC II's. For the most recent version of the IMPACT sensor with the lower acceptable limit set shorter than 6 μs, the rejection rate may be slightly lower.

The bipolar ratio is normally set to 1.0 as the acceptable upper limit. This criterion is effective only for –GC strokes. The evaluated value of this parameter is relatively large and is over the limit in 7 out of 39 –GC strokes, or 18%.

For a pre-trigger-kibosh defined for the period of 0.3 ms before the onset of the main pulse, only one case of –GC strokes is rejected by this criterion. Initial pulse series, however, of larger amplitude are observed in the period of about 1 ms just prior to the main pulse in –GC strokes as shown in Fig. 2. If the time interval is shorter than the dead time in the signal processing of the sensor, the main pulse will be ignored. Distant sensors, however, without the influence of preceding pulses, the main pulse with lower peak amplitude, shorter rise time and longer zero-crossing time than those observed near the radiation source may detect these strokes. In fact, the DE evaluated for the other larger networks in winter is not as low as that for the Tohoku network.

4. CONSIDERATION

4.1 Classification of CG and GC

Even in winter, -CG strokes retain their original (summer) LEMP waveform characteristics. The

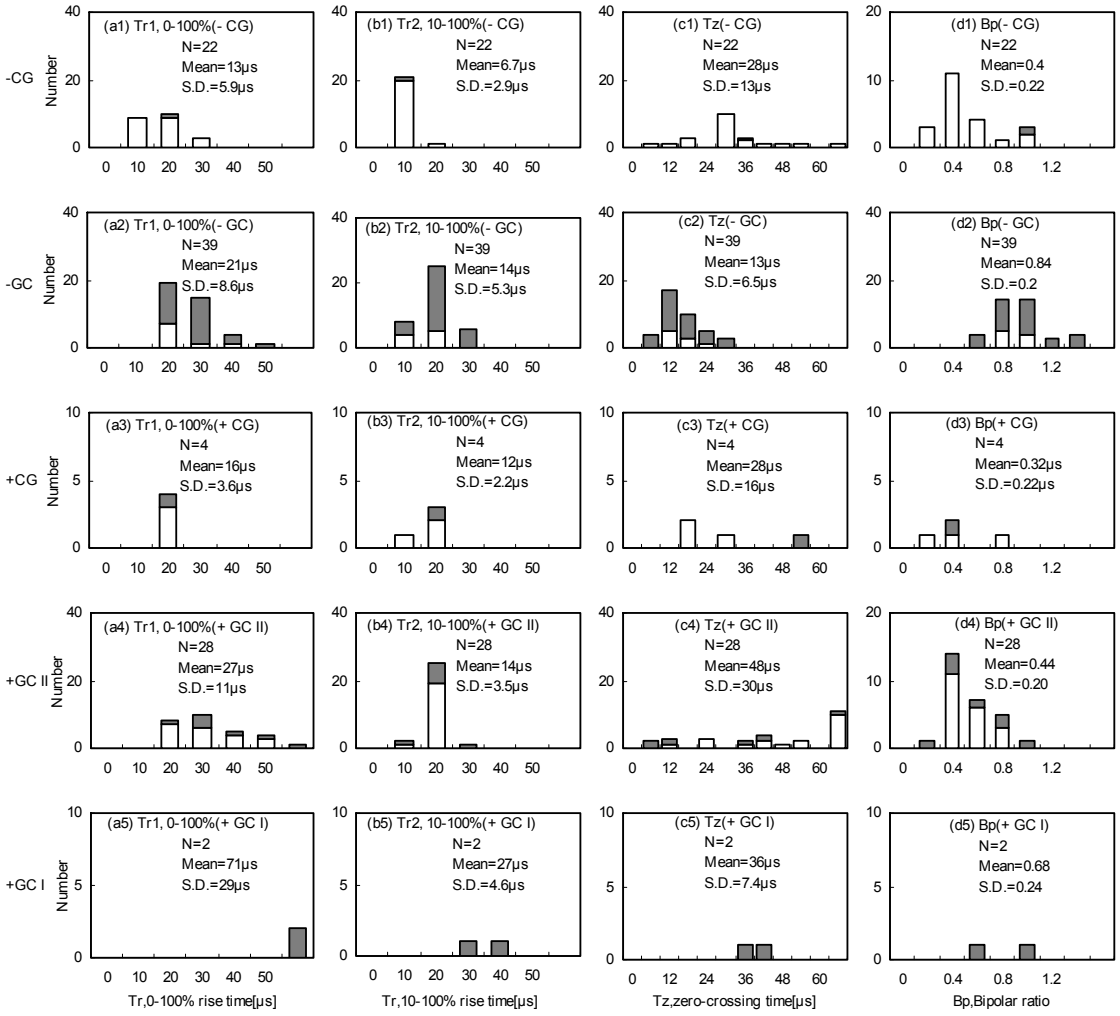

Fig. 4 Histograms of waveform parameters of LEMP associated with the first strokes as (a) 0-100% rise time (Tr1), (b) 10-100% rise time (Tr2), (c) zero-crossing time (Tz), and (d) ratio of initial peak to opposite-polarity overshoot (Bp) in different discharge types of -CG, -GC, +CG, +GC of type II and I sequentially. Note that the scale of the horizontal axis shows the upper limit value of the class, and the shaded bin and white bin stand for the rejected first stroke and the detected one, respectively. Bins on the right edge are the number out of range.

zero-crossing time though is a little shorter and the bipolar ratio is a little larger, which implies the shorter channel bridging between the in-cloud charged region at lower altitude and the ground.

The same condition is applicable to GC strokes in winter. However, the zero-crossing time for +GC strokes distributes in a wide range, and the mean value of that is larger than that for –CG strokes. On the other hand, the shortest portions of the distributions of zero-crossing time are less than 6 μs for either the -GC or +GC II types. The difference of the zero-crossing time between -GC and +GC II indicates that the preceding channel in the cloud, which connects with the leader progressing upward from the ground, for +GC II is much longer than that for –GC. This implies the complex characteristics

of the LEMP waveforms, and the complete classification of +GC strokes into Types I and II will be difficult. Actually, there are many differences between the distribution of the waveform parameters for -CG strokes and –GC strokes, but not between the parameters of +CG strokes and +GC Type II strokes. For the observed fields in this analysis, two-thirds of the positive flashes start with PB, but their polarities are halved and have no correlation with the field waveform features of the discharges that follow them. Therefore it is reasonable to understand the classification of the positive stroke as +CG and +GC II based on the length of the upward connecting leader and its effect. Based on this classification concept, +GC Type I's are at the opposite end of +CG in the category of positive strokes.

Defining the duration of initial discharge (DID), denoted as Ti in ms in the figures below, as the period from the beginning of the significant radiation to the onset of the main pulse, the DID's for positive strokes are a hundred times longer than the DID's of negative strokes as shown in Fig. 5. The distribution of the duration is divided into the longer region for CG strokes and the shorter region for GC strokes regardless of polarity, and the boundary of the distribution is around 1 ms for negative strokes and about 100 ms for positives. The durations for Type I +GC's, less than 10 ms, are around the shortest

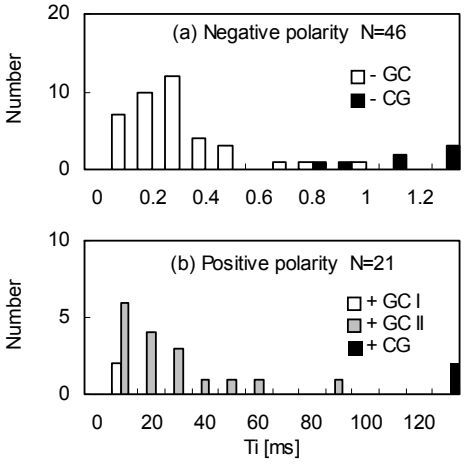

Fig. 5 Histograms of duration of initial discharge (Ti) prior to the main pulse associated with the first stroke in (a) negative polarity and (b) positive polarity. Bins on the right edge are the number out of range.

end of the distribution for Type II +GC strokes.

From the above characteristics, the duration is expected to be useful in discriminating the discharge type of the first stroke. Complete discrimination, however, based only on the duration will still be difficult. This is because that the distributions for different types of discharges are not isolated completely, and discharges generating no significant radiation cannot be observed. However, the DID may be an index of the length of the downward leader for both polarities.

4.2 Waveform parameter and DID

Fig. 6 (a) shows the correlation of the logarithm of peak current, denoted as Ip in kA in the figures below, and the logarithm of DID for negative strokes. The peak currents distribute under about 80 kA for –CG strokes, and in the range of 100-350 kA for –GC strokes. The peak current at the boundary of the –CG and –GC strokes is almost the same as the maximum subsequent stroke peak current observed by the LLS. The peak currents of the negative strokes decrease when the DID is shorter than 0.1 ms, increase until the DID rises to about 0.3 ms, and then decrease approximately inversely proportionally to the logarithm of the DID. For longer DID's, the peak currents seem to be on or just below a line

$$Ip = \frac{100}{Ti} \qquad (1)$$

except for two cases of –GC strokes of larger peak currents.

According to a –GC stroke discharge model proposed by Miyazaki and Ishii, two current pulses of positive and negative polarities flow into the negative horizontal leader channel in the cloud and in the positive upward leader from the ground, respectively. For the model, however, Honma showed that the downward leader channel is not necessarily horizontal. In those models, assuming the negative leader progresses downward with a constant velocity in the cloud, the DID corresponds to the time required for the current pulse to travel from one end to the opposite end. The amplitude of the current pulse flowing along the leader depends on the initial charge density per unit length of the leader. The charge density is more or less unique along the leader except at its ends, if the length is not too short. This indicates the charge density is inversely proportional to the leader length. The above equation derived from the LEMP observations is

consistent with those assumptions and shows the large current for –GC strokes to be due to the shorter downward leader with higher negative charge density. The sole difference of the initiation condition of –GC's from -CG strokes is the high field enhanced by the upward leader penetrating the negatively charged region of the cloud. The leader length, however, corresponding to the peak current of 20 kA is 1 km when the leader velocity is assumed to be 0.2 km/ms based on optical ground observations by other researchers. One of the estimated shorter leader lengths may be due to an end effect at the downward leader tip.

Fig. 6 (b) shows the correlation of pulse width, defined as the sum of the 10-100% rise time and zero-crossing time, with the logarithm of DID for negative strokes. The pulse widths increase with the DID up to about 0.3 ms, and then decrease gradually. The feature is similar to that of the peak current. The width of the field pulse associated with the current traveling along the channel depends on the length of the channel. The pulse width of about 40 μs is estimated to be the time that the current, leaving the leader junction, takes to travel along the upward leader channel to the ground and back to the top of the channel. The length of the upward leader corresponds to 3 km assuming the current velocity as 150 m/μs.

At the beginning of the PB for a –CG stroke, a unipolar pulse or an asymmetric one, which is sometimes hard to identify due to environmental noise, often follows a symmetric bipolar pulse. At the beginning of the initial discharge for a –GC stroke, a similar symmetric characteristic pulse is observed. Pulse intervals just after the characteristic pulse for –GC strokes seem to be in the range of 30-50 μs, which is a little longer than the range for –CG strokes occurring in the same season. The longer pulse intervals in the initial discharge for –GC strokes may indicate the influence of the current pulse traveling along the upward leader from the ground to the leader connection process location.

Around the DID of 0.1 ms, the peak current of the main pulse seems to be at the minimum value for –GC as shown in Fig. 6 (a). There is a positive correlation, however, between the maximum peak amplitude of the pulses in the initial discharge and the main pulse for DID's shorter than 0.3 ms. Therefore, the maximum peak amplitude of the pulses in the initial discharge and the peak amplitude of the main pulse for –GC strokes are attributable to the same factor.

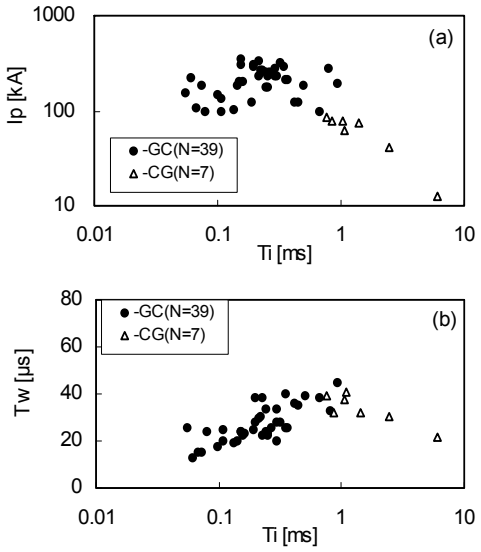

Fig. 6 Scatter charts for negative strokes of (a) logarithmic peak current (Ip) and (b) pulse width (Tw), vs. logarithmic DID (Ti).

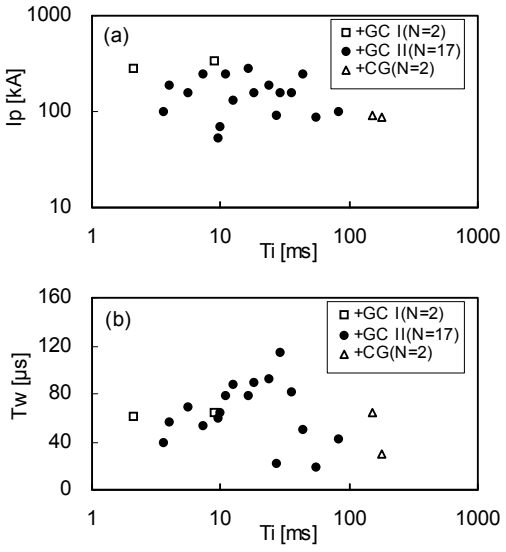

Fig. 7 Scatter charts for positive strokes of (a) logarithmic peak current (Ip) and (b) pulse width (Tw), vs. logarithmic DID (Ti).

Some –GC strokes with DID's of around 0.3 ms seem to have lower pulse widths than the values expected from the distribution of the other data in the figure, although the peak currents are at the high end. In those cases, the main pulse seems to be a bipolar pulse superimposed by a damping oscillation whose duration is shorter than that of the main pulse. The oscillation begins at the first peak identified as the peak corresponding to the return stroke in the analysis and seems to make the subsequent peaks, and also influence the zero-crossing time and the opposite peak. The characteristic oscillation is thought to be generated by the current pulse shuttling in the higher conductive part of the channel around the junction of the leaders.

Fig. 7 (a) shows the correlation of the logarithm of peak current and the logarithm of DID for positive strokes. The peak currents of +GC's and +CG's are at the large and small ends, respectively, of the range over which the +GC II strokes are distributed. The peak currents seem to decrease slightly with the logarithm of DID.

Fig. 7 (b) shows the correlation of the pulse widths with the logarithm of DID for positive strokes. The pulse width increases in proportion with the DID up to about 30 ms, and then decreases rapidly. A portion of the rapid decrease of the pulse width may reflect the decrease in the length of the upward leader from the ground, which is the altitude of the upward leader.

5. SUMMARY

The performance of the IMPACT sensor network in the Tohoku region in winter was evaluated in this paper referring to the study of winter lightning in the coastal area facing the Sea of Japan.

The detection efficiency is 62% for lightning flashes, but decreases to 56% for first strokes. Classifying the first strokes by discharge types, the detection efficiencies are 23% for –GC strokes, and 67% for +GC strokes. These results show that the lower detection efficiency is due to the upward lightning that is peculiar to the coastal area of the Sea of Japan in winter.

GC strokes account for 70% of the entire group of investigated strokes, and rejected GC strokes also account for 95% of all rejected strokes. This indicates the importance of GC strokes, especially in negative polarity, in lightning detection in winter.

In analyzing the LEMP waveforms, it was found that the rejection is caused by the influence of the field pulses prior to the main pulse on the signal processing in the IMPACT sensor, and an incompatibility of the characteristics of the LEMP waveform with the waveform discrimination criteria.

From this analysis, the need for a new sensor with improved detection efficiency for GC strokes is clear.

References

K. L. Cummins, M. J. Murphy, E. A. Bardo, W. L. Hiscox, R. B. Pyle, and A. E. Pifer: A combined TOA/MDF technology upgrade of the US National Lighting Detection Network: J. Geophys. Res. Vol. 103 (D8), pp. 9035-9044 (1998)

K. Shinjo, T. Wakai, T. Sakai, and M. Ishii: Accuracy of LLP System and Lightning Frequency Map Evaluated from Transmission Line Faults, T. IEE Japan, Vol. 117-B, No. 11, pp. 1448-1457 (1997) (in Japanese)

M. Ishii, M. Saito, F. Fujii, J. Hojo, M. Matsui, N. Itamoto and K. Shinjo, "LEMP from lightning discharges observed by JLDN", IEEJ Trans. on Power & Energy, vol. 125, no. 8, pp.765-770 (2005).

M. Ishii, "Electromagnetic fields associated with lightning discharges in winter," IEEJ Trans. on Power &Energy, vol. 127, no. 12, pp.1253-1257 (2007).

M. Saito, M. Ishii, M. Matsui, and N. Itamoto, "Spatial distributions of high current lightning discharges in Hokuriku area in winter", IEEJ Trans. on Power & Energy, vol. 127, no. 12, pp.1325-1329 (2007).

M. Ishii, and M. Saito, "Lightning electric field characteristics associated with transmission-line faults in winter", IEEE Trans. Electromagnetic compatibility, Vol. 51, No. 3, pp. 459-465 (2009).

N. Honma, F. Suzuki, Y. Miyake, M. Ishii, and S. Hidayat: Propagation effect on field waveforms in relation to time-of-arrival technique in lightning location, J. Geophys. Res. Vol. 103 (D12), pp. 14141-14145 (1998)

N. Suzuki, E. Satoh, N. Honma, and M. Ishii: Electromagnetic and optical observation of winter lightning on the coast of the Sea of Japan, Proc. V SIPDA, Sao Paulo-Brazil, pp. 18-22 (1999)

S. Miyazaki, M. Saito, and M. Ishii: Reproduction of features of electromagnetic field waveforms associated with upward lightning discharges, 2006 National Convention Record IEE Japan, No. 7-130 (2006) (in Japanese)